"Shock Waves in Condensed Matter"
Ed. Y.M. Gupta, Plenum, NY, 1986.

MODELING OF INSTABILITY AT THE TIP OF A SHEAR BAND

Marc A. Meyers and Shinhou Kuriyama*
Center for Explosives Technology Research
New Mexico Institute of Mining and Technology
Socorro, New Mexico 87801

* Permanent Address:
Institute of Physical and Chemical Research
Wako, Saitama, Japan

INTRODUCTION AND ASSUMPTIONS

The present work focusses on the tip of the shear band, and assumes that the critical phenomena dictating the propagation or arrest of a shear band occur at the tip. This approach is analogous to fracture mechanics in which the crack tip is the region where the relevant processes are taking place, while the crack surfaces are merely the product. The driving energy for the extension of the tip comes from an increase of the imposed displacement, which generates shear stresses and strains. In the analysis presented in this paper the plastic deformation ahead of a shear band is calculated as a function of imposed displacement. A number of assumptions are required to render the problem tractable. The principal assumptions are given and justified below.

a) Negligible flow stress in shear band (behind the tip). Post-deformation measurements have shown that the hardness in the shear band can be very high and often exceeds that of the surrounding material. However, during the process of propagation, plastic deformation is highly localized in the shear-band region, leading to significant temperature increases. Temperatures can approach and possibly exceed the melting point.

b) An adiabatic stress-strain curve represents the plastic deformation process. An elasto-plastic model that would incorporate these variables and also include heat transfer would be exceedingly complex. Since plastic deformation is occurring at a high strain rate, the assumption of adiabaticity is a reasonable one. The use of an adiabatic stress-strain equation was introduced by Olson et al[1] and greatly simplifies computer calculations, allowing one single equation to represent the behavior of the material over a temperature range up to the melting point; the strain rate is assumed constant. For the model presented here the adiabatic stress-strain curve for quenched and tempered HY-TUF steel obtained by Olson et al.[1] is used; the computational predictions are compared with those of an isothermally deformed material.

c) The body is assumed to be in quasi-static equilibrium throughout the deformation process. As such, wave-propagation effects are absent. In order to express the dynamic movement of the body, the stresses are assumed to increase along the adiabatic stress-strain curve (thus, thermal conductivity is not considered) at the high imposed strain rate.

The adiabatic stress-strain curves are characterized by initial work hardening followed by work softening; a plastic instability strain defines the bounds between the two regimes. For the model herein developed, the adiabatic stress-strain curve for a high strength steel determined at a strain rate of $\dot{\gamma} = 10^2\ s^{-1}$ in a torsion test by Olson et al.[1] was used; it is shown in Fig. 1.

Converting Olson et al.'s [1] equation into effective stress versus effective strain:

$$\bar{\sigma} = \bar{\sigma}_o\ (1 + \alpha\bar{\varepsilon}_p)\ \exp(-\beta\bar{\varepsilon}_p) \qquad [1]$$

where $\bar{\sigma}_o = 1588.3$ MPa, $\alpha = 13.6$, $\beta = 7.24$, $\bar{\varepsilon}^i_p = 0.0646$, and $\bar{\sigma}_{max} = 1868.9$ MPa. The material constants for elastic deformation are E = 206.7 GPa (Young's modulus) and $\nu = 0.28$ (Poisson's ratio). In order to compare the propagation of the shear band under an adiabatic condition with the progressive deformation produced under conditions where no instability occurs, a work hardening curve shown by the broken line (Fig. 1) was developed. It simulates the isothermal behavior of the material, if the assumption that instability is generated by thermal softening is a correct one. Up to the instability strain γ^i_p it is very close to the adiabatic curve. Beyond instability, the two curves diverge markedly, with the work-hardening curve being represented by:

$$\bar{\sigma} = 2240\ (\bar{\varepsilon}_p + 0.005)^{\,0.0649} \qquad [2]$$

These assumptions allow the problem to be modeled by the finite-element method for an elasto-plastic material. The mechanical behavior of the material is assumed to obey the von Mises flow criterion and the incremental theory of Prandtl-Reuss. Deformation of the rectangular body is treated as a plane-strain problem where displacements are given as the boundary condition. The form of elements is triangular, and the displacement function is expressed by a linear polynomial. The adiabatic stress-strain curve given by Equation 1 is used as a constitutive equation in the present code.[2-5]

Metallographic observations indicate that the band thickness, in steels, is in the range 1-3 μm. In the model developed herein the band width was assumed to have a thickness of 20 μm. The material within the band is assumed to have zero strength; the extremity of the band is taken to be approximately semi-circular. Figure 2(a) shows the mesh used to analyse the stresses and strains in the extremity of the shear band. The shape is a rectangle with a width of 400 μm and a length of 500 μm. The shear band is represented by a notch with a semi-circular extremity with a 10 μm radius (BAB') in Figure 2 (a); the notch has a depth of 60 μm and a width of 20 μm. The mesh contains 318 elements and 176 nodal

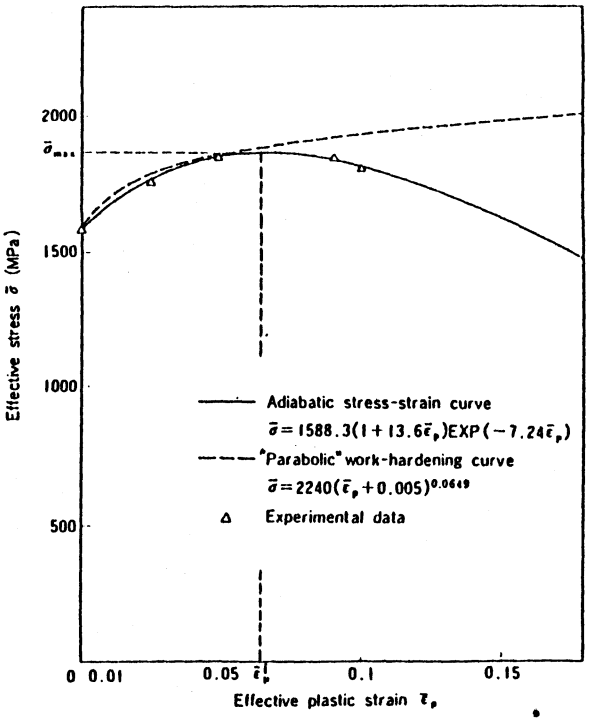

Fig. 1. Effective stress-strain curves for HY-TUF steel in quenched and tempered condition.

points. The shear band is considered to propagate into an infinite material in the x-direction, so that the displacements in x-direction given along a boundary DED' vary linearly as shown in the Figure 2(b) and its boundary condition in y-direction is fixed.

MODEL PREDICTIONS

Figure 3 shows the isostress and isostrain fields developed after a displacement d is given. The stresses and strains marked along the lines are effective values. It can be seen that, although the stress level is fairly high in the whole body (1588-1869 MPa), the plastic strain is concentrated on a narrow band ahead of the notch tip. A thicker solid curve in Figure 3 shows a contour line of $\bar{\sigma}$ =1869 MPa and $\bar{\epsilon}_p$ =0.0646; these values correspond to the maximum stress $\bar{\sigma}_{max}$ and the instability strain $\bar{\epsilon}_p$ at the transition point on the adiabatic stress-strain curve. The stress outside the contour line shown by the solid curve increases with increasing plastic strain due to strain-hardening; however, the stress inside the contour line decreases with increasing plastic strain due to strain-softening. This behavior is shown explicitly in Figure 4(a), where the distributions of stress and plastic strain are shown only in the vicinity of the notch tip. The region contained within the isostress line ($\bar{\sigma}$ =1869 MPa) is considered to correspond to the shear band. In order to compare the propagation of shear band with the progressive deformation produced in a material which has no instability region, the deformation of the notched body is determined for the monotonic work-hardening curve, represented by Equation 2. Figure 4(b) shows the distribution of effective stress and plastic strain near the notch in the parabolic work-hardening material. The deformation of the body and the distributions of stress and strain are almost the same as those in the

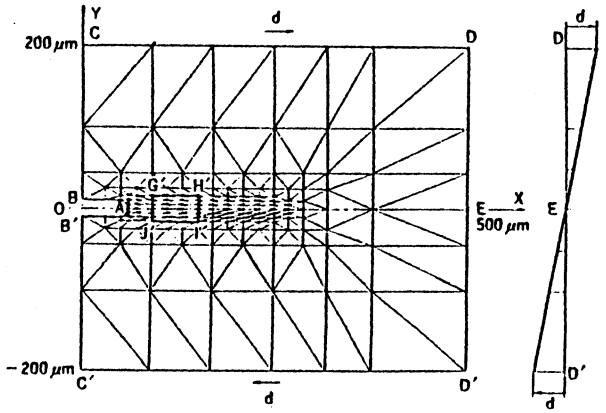

Fig. 2. Mesh division used for sample shear deformation; (a) notch in a rectangular body; (b) boundary displacements imposed along boundary DED.

material of the adiabatic curve except in the vicinity of the notch tip. The isostrain line for $\bar{\varepsilon}_p = 0.0646$ is shown by a solid curve in Figure 4(b); this value is equal to the instability strain $\bar{\varepsilon}^i_p$ of the adiabatic curve. The stress inside the contour line shown by the solid curve increases with increasing plastic strain. This behavior is the same as that outside the contour, but opposite to that of the adiabatic curve. This contour line reaches a distance of 50 μm from the notch tip when the tangential displacement is 6.87 μm. The concentration of strain within the $\bar{\varepsilon}^i_p = 0.0646$ isostrain line, with the attendant reduction of stress, is the critical feature responsible for the propagation of a shear band. By increasing the imposed displacement d, this behavior becomes more and more pronounced; the stress within the instability strain contour line will decrease as d is increased. This drastic difference between adiabatic and isothermal deformation within the $\bar{\varepsilon}^i_p = 0.0646$ envelope contrasts with the nearly identical isostress and isostrain contours outside the envelope. This shows that the overall stress distribution is very similar and explains the localization of the shear along a narrow band.

In order to more clearly assess the effect of the increasing tangential displacement d on the plastic strain distribution along the symmetry axis OE, the plot shown in Figure 5 was made. The symmetry axis OE is indicated by X^1X^3 in Figure 5. The dashed lines represent the isothermal (work-hardening) behavior, while the full lines indicate the adiabatic behavior. At imposed displacements below 3.60 μm, the two conditions deform identically. As d is increased, the plastic shear strain increases at a faster rate for the adiabatic than for the isothermal curve. The difference is highest at the notch tip. The length of the instability region is indicated as S in Figure 6. This region is defined as the length of the $\bar{\varepsilon}^i_p = 0.0646$ envelope for purposes of comparison with the work-hardening curve. Again, the lengths S show marked differences for the two cases beyond a critical displacement d. The length of the instability region S increases very rapidly with increasing displacement d for the adiabatic behavior. Attempts were made at increasing the displacement d further, but serious problems arose regarding the divergence of the solution. Therefore, it was not possible to analyse the full range of the adiabatic stress-strain curve. However, the

trends shown in Figures 3-6 can only accentuate themselves as displacement d is increased.

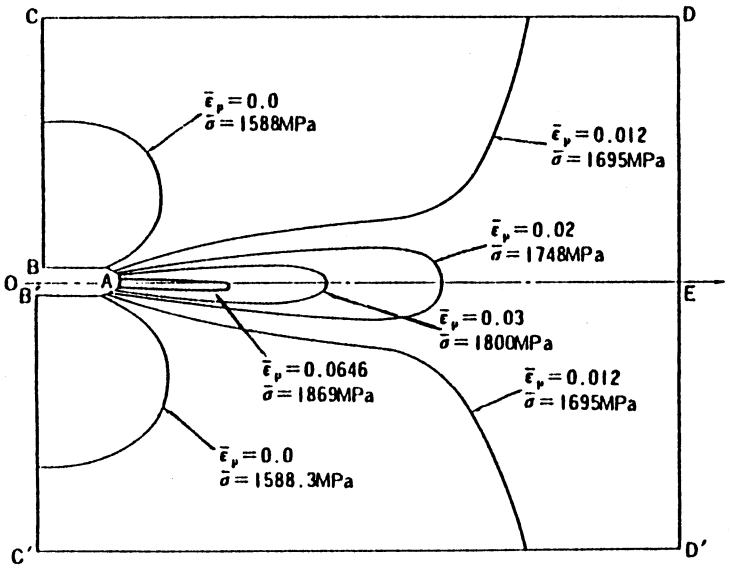

Fig. 3. Isostress (σ) and isostrain ($\bar{\varepsilon}_p$) contour lines in materials with adiabatic stress-strain curve.

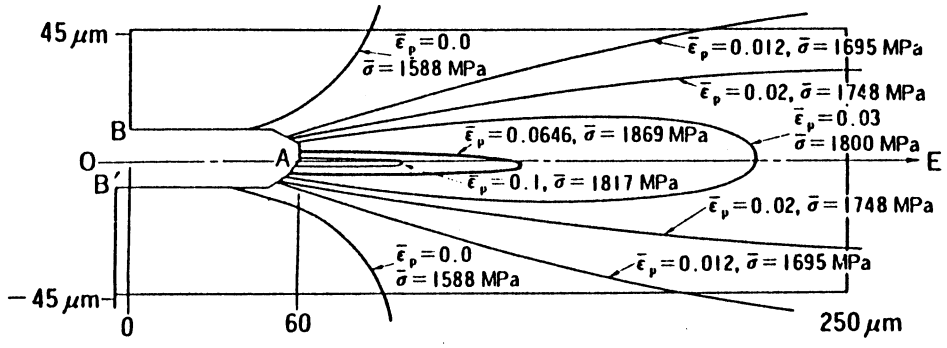

Fig. 4(a). Isostress ($\bar{\sigma}$) and isostrain ($\bar{\varepsilon}_p$) contour lines near the notch in material with adiabatic stress-strain curve. Shear band is produced inside an envelope of solid line $\varepsilon_p^i = 0.0646$.

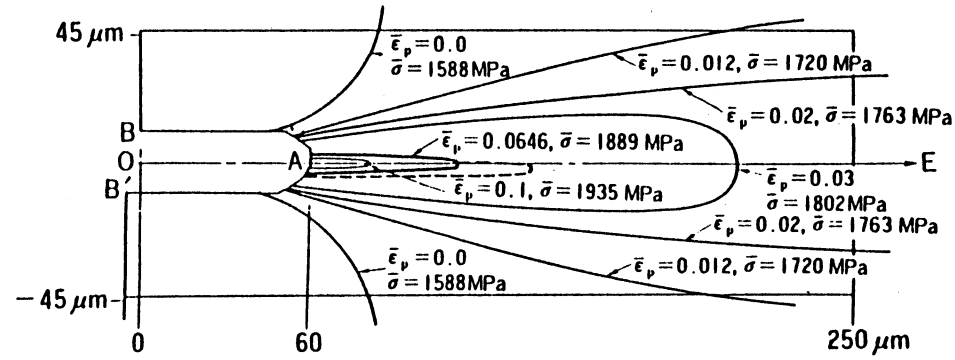

Fig. 4(b). Isostress ($\bar{\sigma}$) and isostrain ($\bar{\varepsilon}_p$) contour lines near the notch in material with workhardening curves.

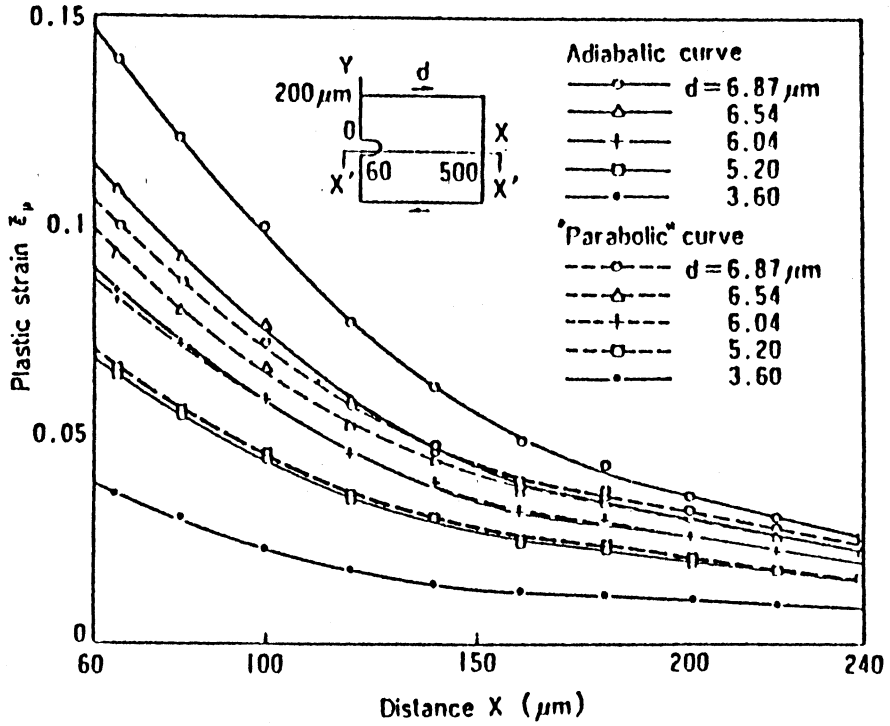

Fig. 5. Comparison of plastic strain distributions along x^1x^1 between material with adiabatic stress-strain curve curve and material with monotonic work-hardening curve.

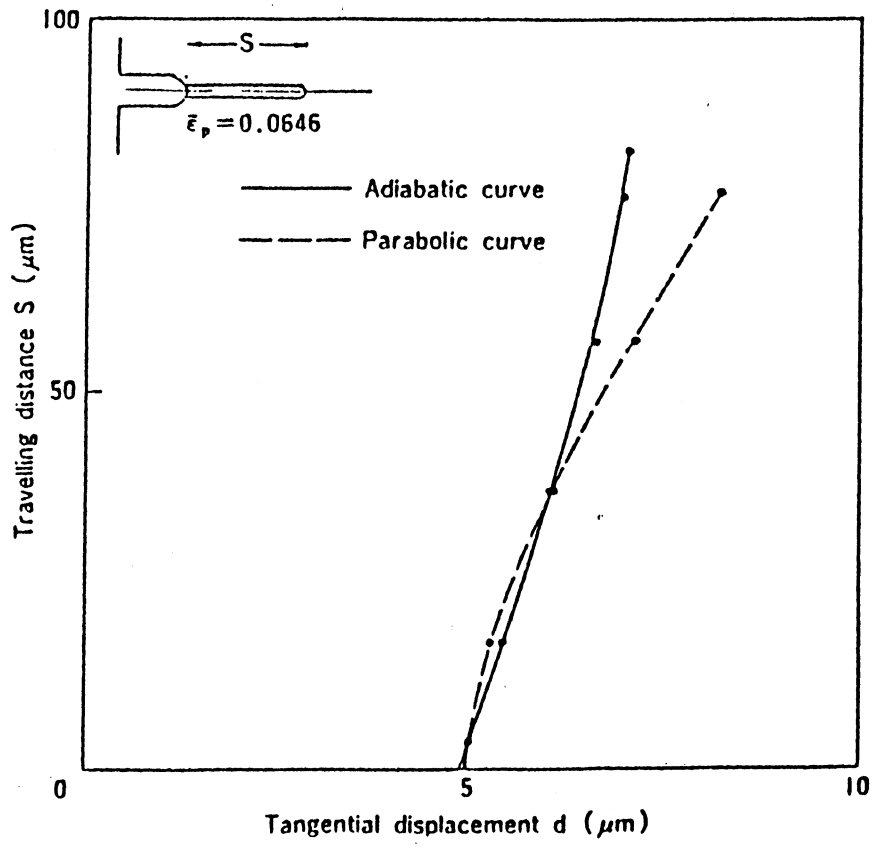

Fig. 6. Lenght of shear band for adiabatic stress-strain curve compared with corresponding distance S for monotonic work-hardening curve.

ACKNOWLEDGMENT

The authors wish to thank Mr. K. Miyauchi (The Institute of Physical and Chemical Research, Japan) for valuable discussions, and Dr. J.L. Swedlow (Carnegie-Mellon University) for permission to use the code. This research was supported by NSF Grant 8115127 and by the Center for Explosives Technology Research.

REFERENCES

1. G.B. Olson, J.F. Mescall, and M. Azrin, in: "Shock Waves and High-Strain-Rate Phenomena in Metals," M.A. Meyers and L.E. Murr, eds., Plenum, New York, (1981), p. 221.
2. J.L. Swedlow, Computers and Structures, 3:878 (1973).
3. S. Kuriyama, H. Hayashi, and S. Yoshida, in: "Proceedings of the 4th International Conference on Production Engineering," Tokyo, (1980), p. 38.
4. Y. Yamada, "Applications of the Finite Element Method," Tokyo, p. 149 (In Japanese).
5. O.E. Zienkiewicz, "The Finite Method in Engineering Science," McGraw-Hill, London, England, p. 50.